The intrinsic exchange bias effect in the $LaMnO_3$ and $LaFeO_3$ compounds

Abd El-Moez A. Mohamed[*a,b], Pablo Álvarez-Alonso[c], B. Hernando[c]

[a] School of Metallurgy and Materials, University of Birmingham, Birmingham, United Kingdom B15 2TT.
[b] Department of Physics, Faculty of Science, University of Sohag, Egypt 82524.
[c] Department of Physics, Faculty of Science, University of Oviedo, Spain 33007.

Abstract

This work aims to investigate the intrinsic exchange bias (EB) of the $LaMnO_3$ and $LaFeO_3$ compounds. The magnetisation dependant temperature shows an anomalous behaviour that is coherent with the coexistence of the ferromagnetic (FM) and the AFM phases. The existence of the FM component is confirmed by the thermal variation of the magnetisation reciprocal, as the specimen describes a Curie-Weis behaviour above 160K with a Curie temperature of 110K. In addition, the magnetic hysteresis loops at low temperatures correspond to a FM-like behaviour. The spin coupling between the FM-AFM phases leads to the EB effect in $LaMnO_3$ and $LaFeO_3$ single phase compounds, where they achieve maximum EB values of -1124Oe and 2343 Oe, respectively. The EB effect suppresses with the partial substitution of La^{3+} by Ba^{2+} due to the dominance of the FM phase and the absence of the FM/AFM coupling as a result of the decrease in the AFM component. Also, the magnetocaloric effect of the pristine and doped $LaBaMnO_3$ was investigated. Where the $LaMnO_3$ shows magnetic entropy change (ΔS) of 0.42J/kg.K with an adiabatic temperature change (ΔT_{ad}) of 0.1k. These values are improved in the doped composite to 1.3J/kg.K and 0.4K due to the dominant FM.

Keywords: Manganites; Magnetic properties; Exchange bias; Magnetocaloric effect; rare earth alloys and compounds.

[*]**Corresponding author: a.a.m.a.hussein@bham.ac.uk**

1. Introduction

The exposure of a ferromagnetic (FM) system to a cyclic magnetic field leads to energy storage in this system because of the irreversible domain rotation [1]. In a pure FM system, the hysteresis loop (HL) is symmetric around the origin, which is interesting for several applications such as data storage [2]. In some inhomogeneous/multilayered FM-AFM systems, the HLs were found to be asymmetric, especially when the system is cooled down in an external applied magnetic field. This asymmetry appears as a shift in the magnetic hysteresis loops along the magnetic field axis and this shift is known as the exchange bias (EB) [3]. This effect occurs due to the FM-AFM coupling and it is interesting for spin dependant technological applications such as read/write spintronic heads [4] and magnetic sensors [5]. EB has been observed for the first time in multi-layered structures such as Fe-Fe_3O_4 [6], and then in heterostructure and artificial interface systems such as $LaNiO_3$-$LaMnO_3$ superlattices [7]. However, the magnetic inhomogeneity of these systems is not repetitive as it is sensitive to the chemical composition [8]. Recently, the EB has been observed in some single phase materials such as Sr_2YbRuO_6 and the effect was attributed to the Dzyaloshinsky– Moria [9]. Similarly, the intrinsic EB effect has been observed in some single phase manganites such as $NdMnO_3$ [9] and $Pr_{0.33}Ca_{0.67}MnO_3$ [10] and has been attributed to the phase separation phenomenon [10]. For example, the FM/AFM phase separation in $Pr_{0.33}Ca_{0.67}MnO_3$ compound can be tuned via controlling the doping ratio that shows AFM ordering, however, there are induced small inclusions of FM nanodomains that couples with the AFM main phase [10].

Manganites have shown also a high magnetocaloric effect (MCE), where it shows a high magnetic entropy change under the effect of an applied magnetic field. This is besides the environmental friendly effects such as chemical stability, low cost and nontoxic effects. These outstanding features have drawn the attention in investigating manganities as magnetic refrigerant materials as an alternative to the Gd based alloys, which are the benchmark in magnetic refrigeration technology [11]. For instance, the bulk LaCaMnO shows a magnetic

entropy change (ΔS) of 7J/kg.K, which is larger than the pure Gd [11]. Accordingly, the aim of this work is to investigate the intrinsic EB effect and the magnetocaloric effect of the $LaMnO_3$, $LaFeO_3$ compounds and their Ba^{2+} doped compounds for magnetic spin based applications and magnetic refrigeration technology.

2. Experimental

The $LaMnO_3$ (LMO), $LaFeO_3$ (LFO), $La_{0.8}Ba_{0.2}MnO_3$ (LBMO) and $La_{0.8}Ba_{0.2}FeO_3$ (LBFO) composites were synthesised by the sol-gel method. Stoichiometric solutions of $LaN_3O_9.6H_2O$, $Ba(OOCCH_3)_2$, $Mn(OOCCH_3)_2 .4H_2O$ and $Fe(NO_3)_2$ were mixed, then citric acid was added to the mixture with volume ratio of 1:1. The colloid was dried, ground and heated two times at 600ºC for 8 hours to ensure the complete evaporate of the organic complexes. The powder was pelletised and sintered at 1200 ºC for 24 hours, then left to cool down gradually to room temperature. The crystal structure was examined at room temperature via the x-ray diffraction technique using Philips X'pert Pro MPD diffractometer with CuK_α radiation (λ=1.54Å). The structural analysis was performed via Rietveld refinement method using the FULLPROF software. The magnetic properties were carried out using a physical properties measurement system (PPMS) quantum design. The magnetisation dependent temperature was measured at 100Oe applied magnetic field, the field cooling hysteresis loops were measured using 2T applied magnetic field and the isothermal magnetisation curves were measured up to 3T applied magnetic field. The direct adiabatic temperature change was measured as reported in [12].

3. Results and discussion

3.1 Structure

The XRD patterns in Fig.1a show a polycrystalline structure with high homogeneity for all samples. The analysis of these patterns shows the Pnma orthorhombic structure for the pristine LMO and LFO compounds, in agreement with the literature [1,13,14]. The orthorhombic distortion was reported in these pristine compounds due to the rich content of

Mn^{3+} and Fe^{3+}, which are active ions for Jahn-Teller orthorhombic distortion [15]. The partial substitution of La^{3+} by Ba^{2+} in LMO and LFO decreases the orthorhombic distortion by inducing the mixed valence state (Mn^{3+}/Mn^{4+}) and (Fe^{3+}/Fe^{4+}), respectively (the ratio of Mn^{3+} and Fe^{3+} decreases) [16]. This improves the crystal symmetry in the LBMO composite that shows a structural transformation to the R3c rhombohedral structure, in agreement with previous works [17]. Nevertheless, the LBFO shows the same Pnma orthorhombic of the pristine compound in agreement with the previously reported results of the $LaCaFeO_3$ [34]. In spite of the same orthorhombic structure of the LFO and LBFO compounds, but the LBFO shows less distortion due to the presence of the Fe^{4+} that is a non-active ion for Jahn-Teller effect [18]. Rietveld refinement profile is presented in Fig.1b for the LMO as an example with the refinement goodness of fitting 2.18.

3.2 Magnetic properties

3.2.1 Magnetisation

Fig.2 shows the magnetisation dependent temperature curves, M(T), for the pristine and doped composites. The pristine LMO compound in Fig.2a shows an antiferromagnetic (AFM) behaviour with Neel temperature (T_N) value of ≈120K. The T_N value is similar to previously published works [19,20] and close to reported by *Aruta et al.* (130K) [21]. The T_N value is lower than the benchmark value in the bulk LMO compound (140K) [20]. This deviation was reported previously in [19,20,22,23] and has been attributed to the change in oxygen level ($LaMnO_{3\pm\delta}$) during the heat treatment process that induces a FM component from the canted spin states that act against the main AFM nature of the compound [20]. On the other hand, the LFO in Fig.2b compound doesn't show any magnetic transition in the measured temperature range due to the high T_N value that approaches 740K [24,25]. These results of the bulk samples are quite different from those obtained in the nanosize compounds due to La vacancies and the core-shell structure [26]. Fig.2a,b shows a hysteresis and discontinuity in the ZFC-FC M(T) curves of the pristine LMO and LFO compounds. This bifurcation in the ZFC-FC curves was

observed in $NdMnO_3$ [27] and reports the presence of a FM component in both pristine compounds [28]. The thermal variation of M reciprocal in Fig.2c confirms the existence of this FM component in the LMO compound, where the M^{-1} changes linearly with T above 160K, suggesting a Curie-weiss behaviour [29] with estimated θ_p value of 110K that means the existence of a FM behaviour below this temperature. More evidence for the FM component in LMO and LFO compounds is provided by the magnetic hysteresis loops (HL) measurements below 110K in Fig.3 that shows a FM like HL. It is worth to mention that the M^{-1} vs T curve for the LFO compound couldn't be assessed due to the limited M(T) measurement below the T_N. Nevertheless, the HL in Fig.3b can confirm the presence of the FM component in the same manner of the LMO. The observed negative magnetic moment of LFO in Fig.2b indicates that the La^{3+} has AFM coupling with Fe^{3+} in the measured temperature range, however, it has been reported that strong magnetic fields can flip the La^{3+} spins, giving rise the positive moment [27,9]. Accordingly, the FM and AFM ordering are coexist in both LMO and LFO compounds below a certain temperature and the magnetic state can be described as a competition between the FM and the AFM interaction. The LMO and LFO have been reported as A-type antiferromagnetic oxides, so, the FM component is more likely to occur due to the spin canting effect [9].

The partial substitution of La^{3+} by Ba^{2+} in LBMO drives the AFM to a strong FM with FM-PM transition at 281K near the room temperature, as seen in Fig. 2a. In contrast, the partial substitution of La^{3+} by Ba^{2+} in LBFO has a smaller effect on the magnetic properties than in the LBMO (see Fig.2b). Where the improvement only is in the positive magnetisation value without any magnetic transition, in agreement with the results of $La_{1-x}NaxFeO_3$ [30], which may locate above the measured temperature range. The change in the magnetic properties due to the introduction of Ba^{2+} refers to the changes in two important factors the structural properties and the magnetic interactions [31]. The pristine LMO and LFO compounds are rich

in Mn^{3+} and Fe^{3+}, respectively, which are active ions for Jahn-Teller orthorhombic distortion [32]. This results in charge ordering effect that leads to A-type AFM structure [32], and the only allowed electron transfer occurs via the dominant AFM super exchange Mn^{3+}-O-Mn^{3+} and Fe^{3+}-O-Fe^{3+} interactions [33]. The partial substitution of La^{3+} by Ba^{2+} induces a mixed valence state in both LBMO and LBFO (Mn^{3+}/Mn^{4+} and Fe^{3+}/Fe^{4+}), which increases the FM double exchange interactions (DE) Mn^{3+}-O-Mn^{4+} and Fe^{3+}-O-Fe^{4+} [33]. The FM DE interactions are responsible for the FM-PM transition in LBMO and the promotion magnetisation promotion in LBFO. In spite of the existence of the mixed valence state in both LBMO and LBFO, but the magnetic properties of the LBMO are more pronounced than the LBFO. This is attributed to the structural properties, where the electron transfer between the Mn-O-Mn in the rhombohedral structure (LBMO) is easier than in the Fe-O-Fe bonds of orthorhombic structure (LBFO) [15].

3.2.2 Exchange bias effect

The magnetic hysteresis loops (HL) at different temperatures for the LMO and LFO compounds were assessed in ZFC and FC (μ_0H=2T) modes. Fig.3 shows the ZFC HL and the inset shows a magnified view for the magnetisation change around the origin. The coercivity (Hc) for both LMO and LFO compounds decreases monotonically with temperature elevation (See Fig.4a,b), for example, the Hc of the LMO compound decreases from 1974Oe at 60K to 624Oe at 100K, while the Hc of the LFO decreases from 1223Oe at 60K to 1108Oe at 300K, in similar behaviour with the results in [34]. The temperature dependence of the Hc confirms the induced FM component as the pinned oriented magnetic domains are frustrated across the anisotropy barrier [35] due to the thermal agitation acquired during the temperature elevation [36]. Cooling down the temperature (below T_c) under the effect of an external magnetic field results in asymmetric HL around the magnetisation axis in comparison with the ZFC mode, revealing the exchange bias (EB) effect as seen in Fig.4c for the LMO compound. The

exchange bias effect was calculated according to the equation $HE=Hc_1+Hc_2$ [27], H_{c1} and H_{c2} are the coercive fields at the descending and the ascending branches of the magnetic HL, respectively.

This shift in HL with magnetic field application is attributed to the stripe domain structure of the FM phase component during the FC process [38]. It is also can be explained in terms of the exchange spring effect [39], where the spins of the AFM phase are polarised by the FM spins, creating a planer domain wall [29]. Fig.4a,b also shows the temperature dependence of EB of the LMO and LFO compounds, respectively, where it increases with decreasing the temperature achieving maximum values of -1124Oe at 60K for the LMO and 2343 Oe for the LFO at the same temperature. These values are comparable with $NdMnO_3$ (2400Oe) [9], the Sm0.5Ca0.5MnO3 (≈1200) [38] and NiMnIn ribbon (≈18Oe) [40]. The exchange bias dependence on temperature can be interpreted by the increase in the FM-AFM coupling with decreasing the temperature as a result of the induced ferromagnetic part [41]. So, the EB effect and Hc are expected to vanish above 110K (the Tc) due to the depletion of the FM canted spins and the pure AFM (below T_N). Introducing Ba^{2+} increases the ferromagnetism in the pristine compounds and decreases the AFM part, so the FM-AFM coupling decreases in a notable way in the doped compound as seen in Fig.4d.

3.2.3 Magnetocaloric effect

The isothermal magnetisation curves, M(H), of the LMO and LBMO composites are presented in Fig.5a,b The magnetic transition is clear from the M(H) behaviour above and below the transition temperature. Where the M(H) curves below the magnetic transition temperature increase sharply with the applied magnetic field then saturates at high fields (Ferromagnetic-like behaviour). Meanwhile above the magnetic transition temperature the magnetisation increases linearly with the applied magnetic field (paramagnetic-like behaviour). The induced Arrott plots in Fig.5c,d were assessed to determine the nature of the magnetic

transition (first order or second order). *Banerji* has reported that the positive slope of Arrott plot curves around the magnetic transition temperature reveals a second order magnetic transition, while the negative slope represents a first order transition [42]. Based on these criteria, both LMO and LBMO show a second order magnetic transition due to the negative slope of Arrott plots.

The magnetocaloric effect was determined by two direct and indirect methods. The indirect method was performed by calculating the magnetic entropy change (ΔS) from the M(H) curves, using Maxwell equation, meanwhile, the direct method was performed via the direct measurement of the adiabatic temperature change. First, ΔS was calculated from the M(H) curves using Maxwell equation $\Delta S(T,\Delta H)=\Sigma(M_i-M_{i+1})/(T_i-T_{i+1})$ [43], M_i, M_{i+1} are the magnetisation values at T_i and T_{i+1} temperatures. The thermal variation of ΔS is presented in Fig.6a, the LMO compound shows a maximum ΔS (ΔS_{max}) of 0.42J/kg.K, which is about 25% from the value achieved by *Biswas et al.* at 5T [44] and larger than the $La_{0.67}Sr_{0.33}MnO_3$ nanoparticles (ΔS_{max}=0.32 J/kg.K) [45]. The ΔS_{max} of the LMO compound is improved in the doped composite LBMO to 1.3J/kg.K, which is quite close to the reported results in [46], and larger than the nano $La_{0.4}Ca_{0.6}MnO_3$ (ΔS_{max}=0.13J/kg.K) [47]. The direct measurement of the adiabatic temperature change (ΔT_{ad}) is presented in Fig.6b, where the pristine LMO shows a maximum value of 0.11K, which is improved to 0.4K in the LBMO doped composite. The small values of ΔS and ΔT_{ad} refer to the second order transition that weakens the MCE. It is worth to mention that the MCE of the LFO couldn't be considered due to the high magnetic transition temperature that locates out of the measured range.

4. Conclusion

The LMO, LFO, LBMO and LBFO samples were prepared via the sol-gel method. The pristine LMO and LFO compounds show Pnma orthorhombic structure, however the partial substitution of La^{3+} by Ba^{2+} changes the crystal structure of the LBMO to the R3c

rhombohedral structure without any effect on the LBFO that kept the same orthorhombic symmetry. The M(T) curves show the AFM nature of both LMO and LFO, nevertheless, the observed hysteresis between the ZFC and FC curves reveals the coexistence of a FM component. The calculation showed that the FM component exists below 110K in the LMO compound, but it couldn't be assessed in the LFO compound as it locates above the measured temperature range. The existence of the FM component was confirmed by the hysteresis loops measurements below 110K that show a FM-like behaviour. The FM-AFM spin coupling leads to the observed EB effect, where the LMO and the LFO show EB field of -1124 Oe and 2343 Oe, respectively. The introduction of Ba^{2+} ions suppresses the EB effect in the LBMO due to the decrease in the FM/AFM coupling as a result of the FM dominant behaviour. For the MCE properties, the pristine LMO compound shows ΔS_{max} of 0.42J/kg.K and ΔT_{ad} value of 0.1k, meanwhile the LBMO doped composite shows ΔS_{max} value of 1.3J/kg.K and ΔT_{ad} value of 0.4K as a result of the improvement in the ferromagnetism.

References

1- M. S. Selbach, R. J. Tolchard, A. Fossdal, T. Grande, Non-linear thermal evolution of the crystal structure and phase transitions of LaFeO3 investigated by high temperature X-ray diffraction, J.Solid State Chem. 196 (2012) 249-254.

2- K. H. J Buschow. New developments in hard magnetic materials. Rep. Prog. Phys. 54 (1991)1123-1213.

3- J. Nogues, I. K. Schuller, Exchange bias. J. Magn. Magn. Mater. 192 (1999) 203-232.

4- C. Chappert, A. Fert, F. N. V. Dau, The emergence of spin electronics in data storage. Nat. Mater. 6 (2007) 813-823.

5- S. Fukami [1], C. Zhang , S. DuttaGupta , A. Kurenkov , H. Ohno., Magnetization switching by spin–orbit torque in an antiferromagnet-ferromagnet bilayer system. Nat. Mater. 15 (2016) 535-541

6- V. Papaefthymiou, A. Kostikas, A. Simopoulos, D. Niarchos, S. Gangopadyay, G. C. Hadjipanayis, C. M. Sorensen, K. J. Klabunde, Magnetic hysteresis and Mössbauer studies in ultrafine iron particles J. Appl. Phys. 67, 4487 (1990).

7- M. Gibert, P. Zubko, R. Scherwitzl, J. I~niguez, and J.-M. Triscone, Nature Mater. 11, 195 (2012).

8- J D Dutson, C Huerrich1, G Vallejo-Fernandez, L E Fernandez-Outon, G Yi, S Mao, R W Chantrell and K O'Grady, Bulk and interfacial effects in exchange bias systems. J. Phys. D: Appl. Phys. 40 (2007)1293-1299.

9- F. Hong, Z. Cheng, J. Wang, S. Dou, Positive and negative exchange bias effects in the simple perovskite manganite NdMnO3, App. Phy. Let. 101 (2012) 102411.

10- D. Niebieskikwiat, M. B. Salamon, Intrinsic interface exchange coupling of ferromagnetic nanodomains in a charge ordered manganite. Phys. Rev. B 72 (2005)174422–174422.

11- A. Biswas, T. Samanta, S. Banerjee, I. Das, Magnetocaloric properties of nanocrystalline La0.125Ca0.875MnO3 Appl. Phys. Lett., 94 (2009) 233109.

12- P. Álvarez-Alonso, J. López-García, G. Daniel-Perez, D. Salazar, P. Lázpita, J.P. Camarillo, H. Flores-Zuñiga, D. Rios-Jara, J.L. Sánchez-Llamazares, and V.A. Chernenko, Simple set-up for adiabatic measurements of magnetocaloric effect, Key Engineering Materials 644 (2015) 215-218.

13- P. Coppens, M. Eibschutz Acta Crystallogr., 19 (1965). 524-531.

14- P. Norby, I. G. Krogh Andersen, E. Krogh Andersen, The Crystal Structure of Lanthanum Manganate(lll), LaMnO,, at Room Temperature and at 1273 K under N, **J. Solid state chem.** 119 (1995) 191-196.

15- Elemans J. B. A. A., Van Laar B., Van Der Veen K. R. Loopstra B. O., The crystallographic and magnetic structures of La1−xBaxMn1−xMexO3 (Me = Mn or Ti) J. Solid state chem., 3 (1971) 238.

16- Rezlescu E., Doroftei C., Popa P. D. and Rezlescu N., The transport and magnetic properties of La–Pb–Mg–Mn–O manganites at low temperatures J. Magn. Magn. Mater., 320 (2008) 796.

17- Y.C. Liou , Y.R. Chen, Synthesis and microstructure of (LaSr)MnO3 and (LaSr)FeO3 ceramics by a reaction-sintering process, Ceramics International 34 (2008) 273–278.

18- Q.Lin, J. Xu, F. Yang, X. Yang,Y. He, The influence of Ca substitution on LaFeO3 nanoparticles in terms of structural and magnetic properties, J Appl Biomater. & Functional Materials 16(2017)18.

19- V. Markovich,a) E. Rozenberg, G. Gorodetsky, and G. Jung I. Fita, R. Puzniak, A. Wisniewski C. Martin, S. Hebert, and B. Raveau, Vacancies at Mn-sites in LaMn1ÀxO3 manganites: Interplay between ferromagnetic interactions and hydrostatic pressure, J. Appl. Phy. 95 (2004) 7112.

20- S. Chandra, A. Biswas, S. Datta, B. Ghosh, V Siruguri, A K Raychaudhuri, M H Phan, H Srikanth, Evidence of a canted magnetic state in self-doped $LaMnO_{3+}\delta$ (δ= 0:04): a magnetocaloric study, J. Phys.: Condens. Matter 24 (2012) 366004.

21- C. Aruta, M. Angeloni, G. Balestrino, N.G. Boggio, P.G. Medaglia, A. Tebano, B. Davidson, M. Baldini, D. Di Castro, P. Postorino, P. Dore, A. Sidorenko, G. Allodi, R. De Renzi Preparation and characterization of $LaMnO_3$ thin films grown by pulsed laser deposition J. Appl. Phys., 100 (2006) 023910.

22- S. Chandra, A. I. Figueroa, B. Ghosh, M. H. Phan, H. Srikanth, A. K. Raychaudhuri, Phase coexistence and magnetic anisotropy in polycrystalline and nanocrystalline $LaMnO_{3+\delta}$ J. Appl. Phys. 109 (2011) 07D720.

23- P. A. Joy, R. Sankar. S. K. Date J. Phys.: Condens. Matter 14 (2002) 4985.

24- M. Shang, C.T. Zhang, L. Yuan, L. Ge, H. Yuan, H. Feng, Appl. Phys. Lett. 102(2013) 062903.

25- J.W. Seo, E.E. Fullerton, F. Nolting, A. Scholl, J. Fompeyrine, J.P. Locquet, J. Phys.: Condens. Matter 20 (2008) 264014.

26- R. Horyń, A. J. Zaleski, E. Bukowska, A. Sikora, On magnetic properties of LaMnO3±δ phase within its domain, J. Alloys Compds 383 (2004) 80-84.

27- AMu˜noz, J A Alonso‡, M J Mart´ınez-Lope, J L Garcıa-Munoz and M. T. F.Dıazk, Magnetic structure evolution of NdMnO3 derived from neutron diffraction data, J. Phys.: Condens. Matter 12 (2000) 1361–1376.

28- Tokura Y (ed) 2000 Colossal Magnetoresistive Oxides(London: Gordon and Breach)

29- A. Scholl, M. Liberati, E. Arenholz, H. Ohldag, Stöhr, Creation of an Antiferromagnetic Exchange Spring J Phys. Rev. Lett. 92 (2004) 247201.

30- E. Cao, Y. Qin, T. Cui, L. Sun, W. Hao, Y. Zhang, Influence of Na doping on the magnetic properties of LaFeO3 powders and dielectric properties of LaFeO3 ceramics prepared by citric sol-gel method, Ceramics International 43 (2017) 7922-7928

31- I.A. Serrano, C. Pico and M.L. Veiga , Structural characterization, electric and magnetic behaviour of Zn-doped manganites Solid State Sci., 6 (2004) 1321

32- E. O. Wollan and W. C. Koehler, Neutron Diffraction Study of the Magnetic Properties of the Series of Perovskite-Type Compounds [(1−x)La, xCa]MnO3, Phys. Rev. 100 (1955) 545

33- Zener, C., **Interaction between the d shells in the transition metals**81,(1951) 440-444

34- S. E Nadir. Osman · T. Moyo, Temperature Dependence of Coercivity and Magnetization of Sr1/3Mn1/3Co1/3Fe2O4 Ferrite Nanoparticles, J. Supercond Nov Magn 29 (2016)361–366.

35- K. Maaz, A Mumtaz., S.K. Hasanain, M.F Bertino, Temperature dependent coercivity and magnetization of nickel ferrite nanoparticles J. Magn. Magn. Mater. 322 (2010) 2202.

36- Köseglu, Y., Alan, F., Tan, M., Yilgin, R., Öztürk, M., Low temperature hydrothermal synthesis and characterization of Mn doped cobalt ferrite nanoparticles Ceramic Intern. 38 (2012) 3634.

37- F. Huang, X. Xu, X. Lu, M. Zhou, H. Sang, J Zhu, The exchange bias behavior of BiFeO3 nanoparticles with natural core-shell structure, Sci. Rep. 8 (2018)2311.

38- P. Dasgupta1, K. Das, S. Pakhira, C. Mazumdar, S. Mukherjee, S. Mukherjee, A. Poddar, Role of the stability of charge ordering in exchange bias effect in doped manganites, Sci. Rep. 7: (2017)*3220.*

39- K. Alam , K.Y Meng, R. P-Pérez, G. H Cocoletzi, N Takeuchi, A. Foley, F. Yang A. R Smith, Exchange bias and exchange spring effects in Fe/CrN bilayers, J. Phys. D: Appl. Phys. **53** (2020) 125001.

40- T. Sa´nchez , R.SatoTurtelli, R.Gr¨ ossinger, M.L.Sa´nchez, J.D.Santos, W.O.Rosa, V.M.Prida , Ll. Escoda , J.J.Sun˜ol , V.Koledov, B.Hernando,, Exchange bias behaviour in Ni50.0Mn35.5 In14.5 ribbons annealed at different temperatures, J. Magn. Magn. Mater. 324 (2012) 3535–3537.

41- W. H. Meiklejohn and C. P. Bean, New Magnetic Anisotropy Phys. Rev. 102(1956) 1413.

42- S.K. Banerjee, Phys. Lett., 12 (1964), 67.

43- V.K. Pecharsky, K.A. Gschneidner Jr., Magnetocaloric effect from indirect measurements: Magnetization and heat capacity J. Appl. Phys., 86 (1999) 565

44- A. Biswas, S Chandra, M.H. Phan, H. Srikanth, Magnetocaloric properties of nanocrystalline LaMnO3: Enhancement of refrigerant capacity and relative cooling power, J Alloys Compds. 545 (2012) 157.

45- J. Mira, J. Rivas, L.E. Hueso, F. Rivadulla, M.A. Lopez Quintela, Drop of magnetocaloric effect related to the change from first- to second-order magnetic phase transition in La2/3*(*Ca1−xSr*x)*1/3MnO3 J. Appl. Phys., 91 (2002), 8903

46- A.A Mohamed, B. Hernando, M.E.D Garcia, Room temperature magneto-transport properties of La0.7Ba0.3MnO3 manganite, J. Alloys Compds 695 (2017) 2645-2651.

47- W. Tang, W.J. Lu, X. Luo, B.S. Wang, X.B. Zhu, W.H. Song, Z.R. Yan, Y.P. Sun, Magnetoresistance in two-component Ag/Ni nanocompacts J. Magn. Magn. Mater., 322 (2010), 2360

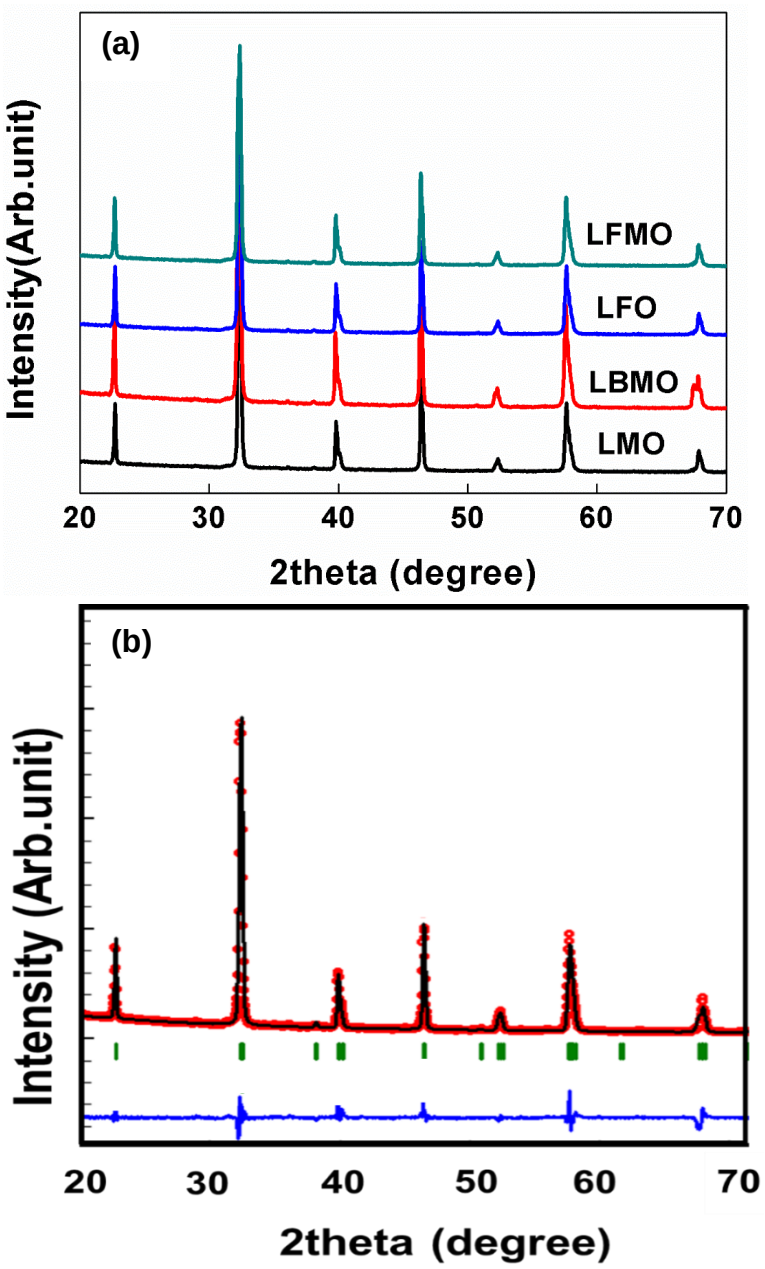

Fig.1: (a) XRD patterns of the LMO, LFO, LBMO and LBF compounds, (b) Rietveld refinement profile for the LMO compound with goodness of fitting (χ^2)=2.18.

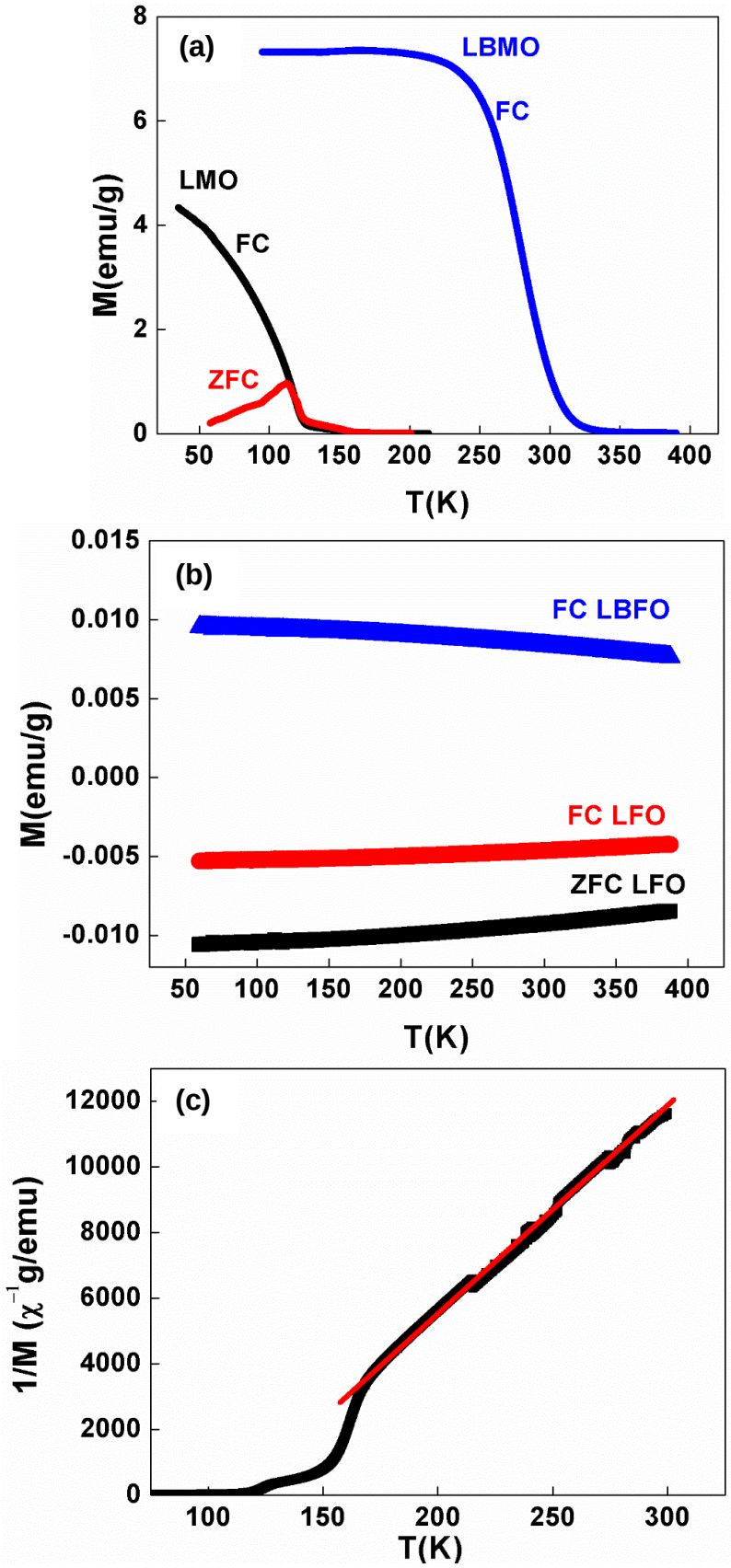

Fig.2: Thermal variation of (a) LMO and LBMO compounds, (b) LFO, LBFO compounds and (c) magnetisation reciprocal of LMO compound.

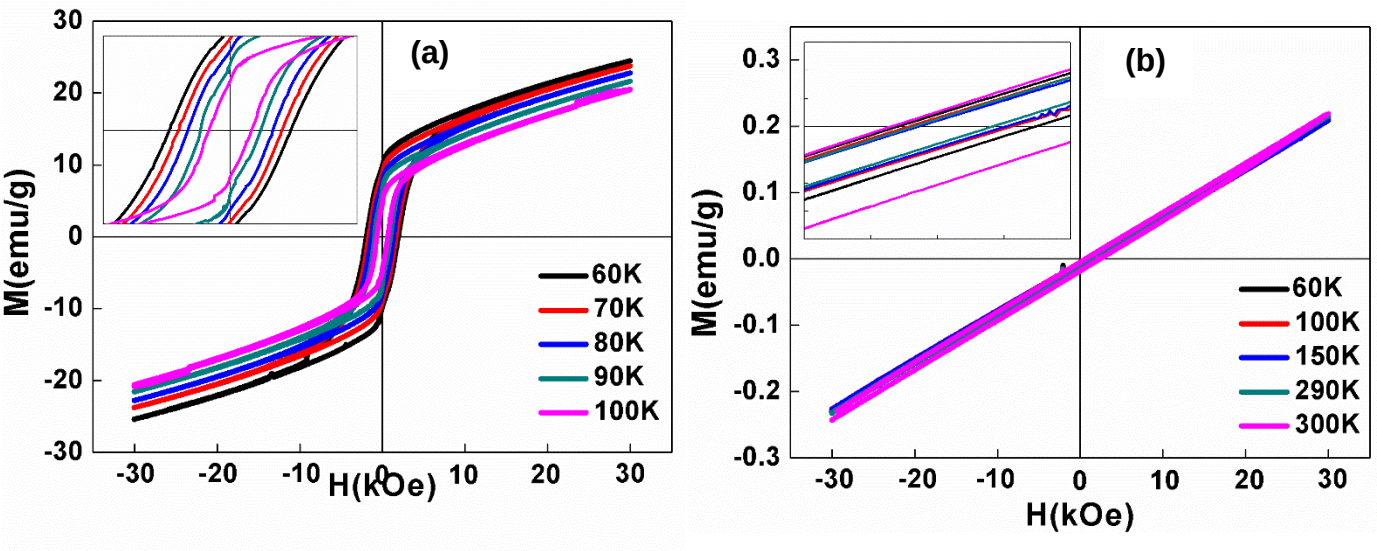

Fig.3: ZFC hysteresis loops at different temperatures for (a) LMO compound, (b)LFO compound.

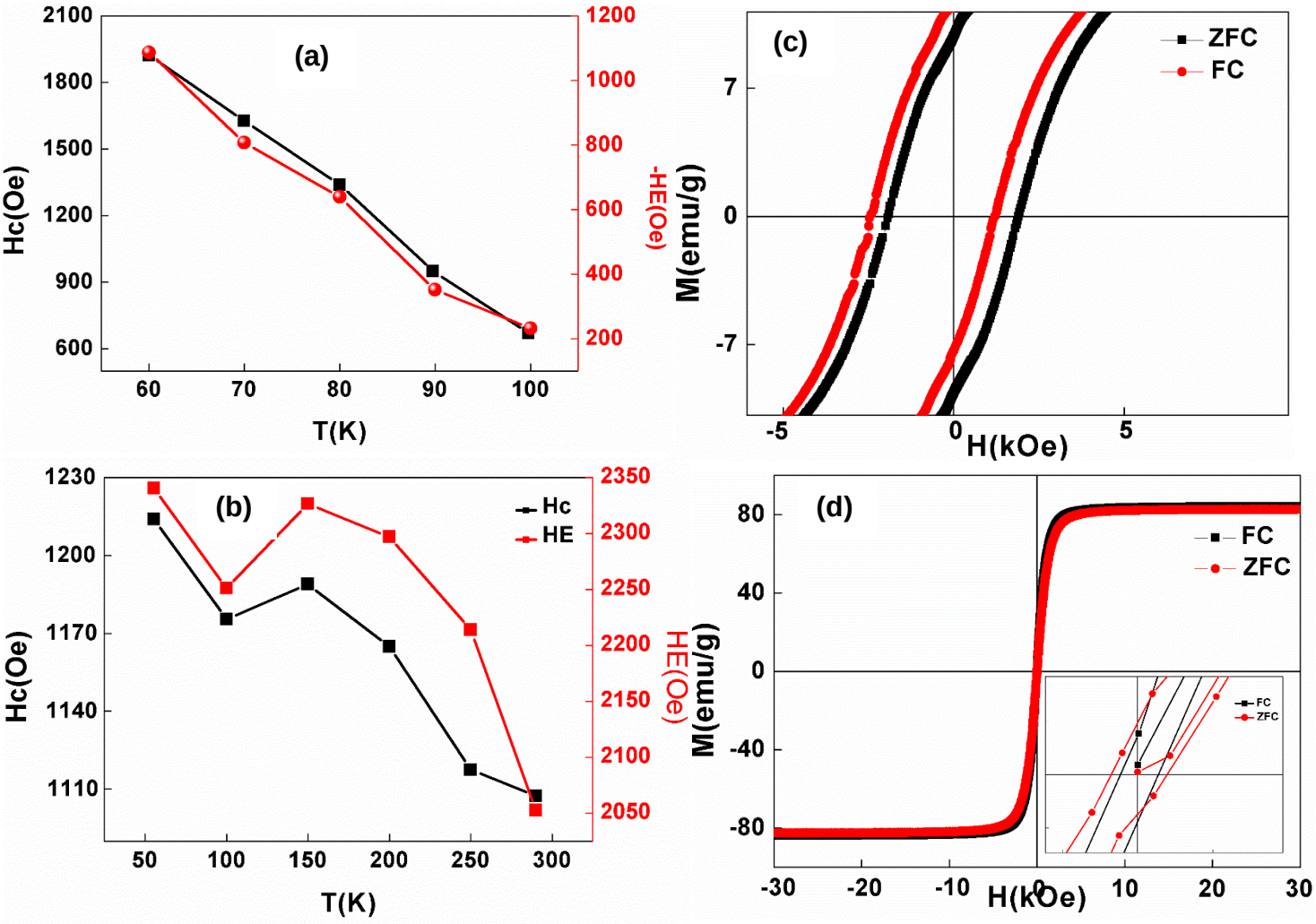

Fig.4: (a,b) Coercivity and exchange bias dependency on temperature for the LMO and LFO compounds, respectively, (c) ZFC-FC hysteresis loop of the LMO around the origin, and (d) ZFC-FC hysteresis loop of the LBMO composite.

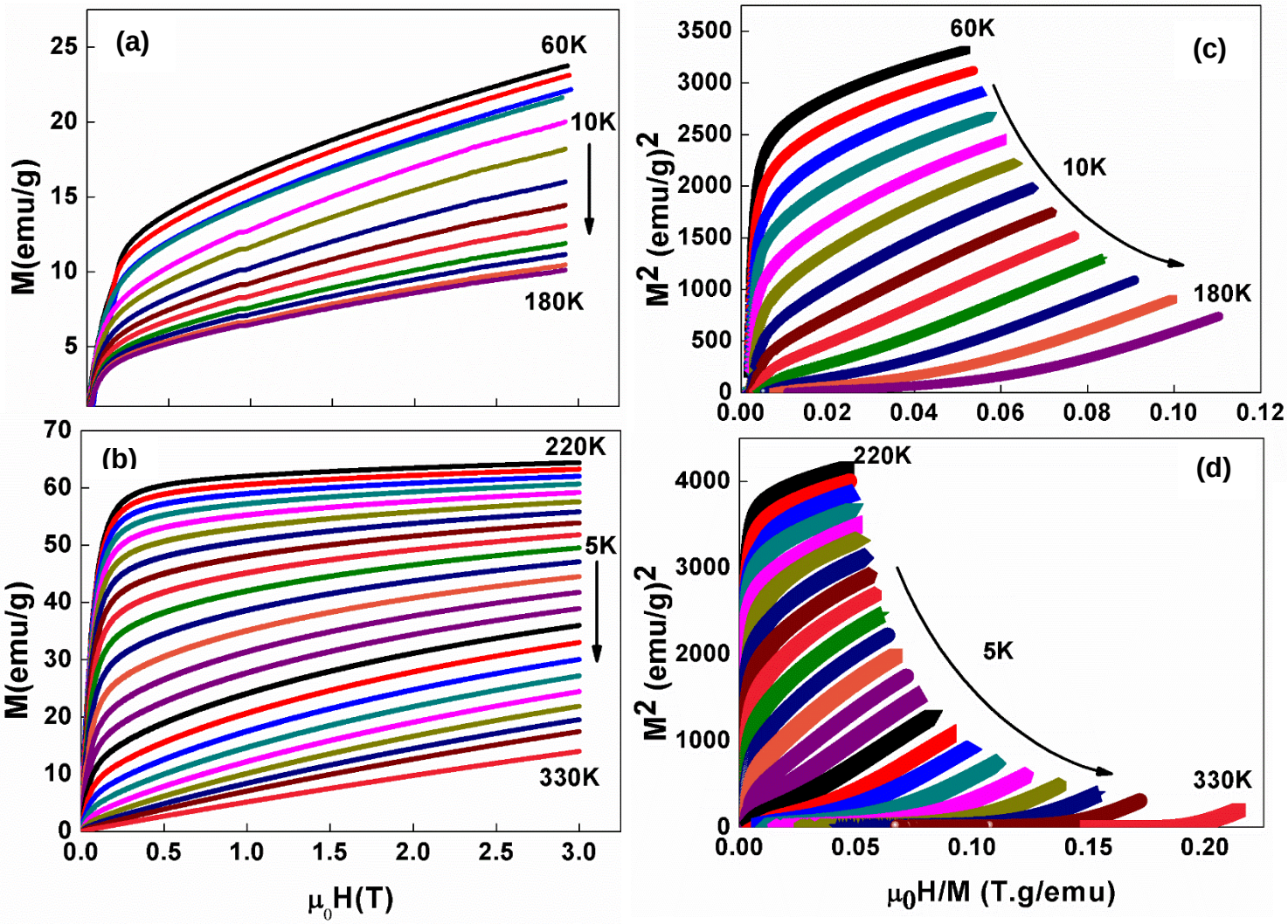

Fig.5: (a,b) the isothermal magnetisation curves of the LMO and LBMO compound, respectively, and (c,d) the relevant Arrott plots.

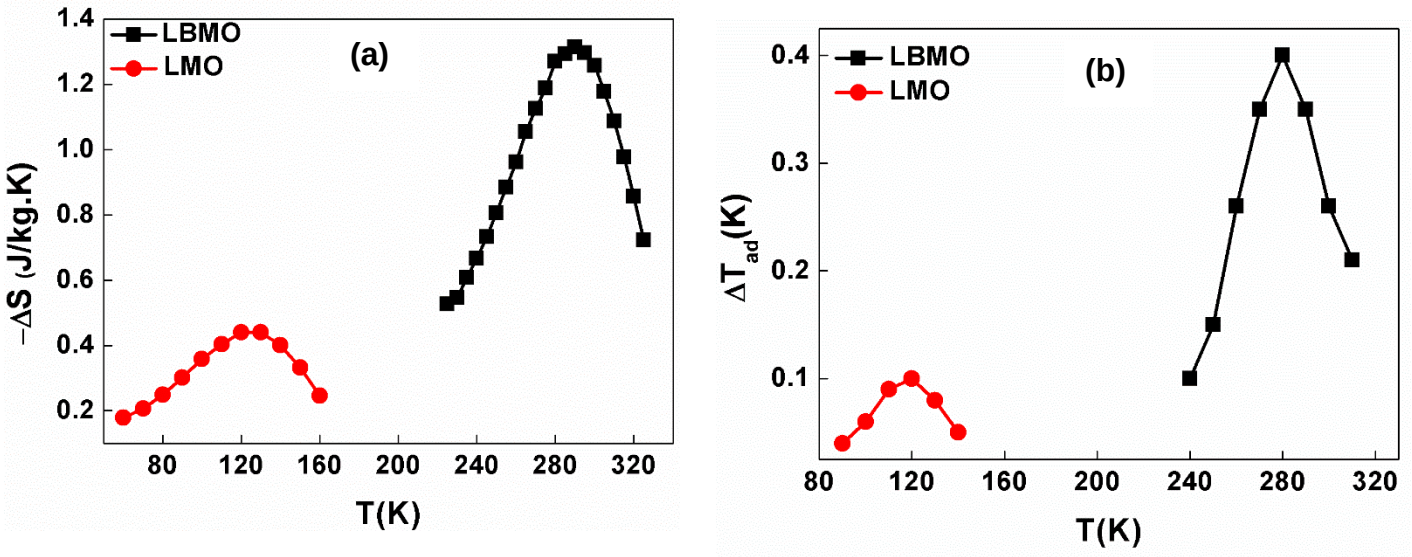

Fig.6: (a,b) ΔS and ΔT_{ad} dependent temperature of the LMO and LBMO composites at $\mu_0 H$=2T.